Edgar L Andreas[1][*], Rachel E. Jordan[1], Peter S. Guest[2], P. Ola G. Persson[3],
Andrey A. Grachev[3], and Christopher W. Fairall[4]

[1]U.S. Army Cold Regions Research and Engineering Laboratory, Hanover, New Hampshire
[2]Naval Postgraduate School, Monterey, California
[3]Cooperative Institute for Research in Environmental Sciences, University of Colorado, Boulder, Colorado
[4]NOAA Environmental Technology Laboratory, Boulder, Colorado

1. INTRODUCTION

The thermodynamic processes within a snowpack respond to the turbulent fluxes of heat, moisture, and momentum at the surface of the snow. Energy budget studies or atmospheric models with snow as the lower boundary almost always estimate these fluxes of momentum (τ) and sensible (H_s) and latent (H_L) heat from a bulk flux algorithm (e.g., Brun et al. 1989; Jordan et al. 1999; Bintanja 2000):

$$\tau = \rho\, C_{Dr}\, U_r^2 ,\qquad (1a)$$

$$H_s = \rho\, c_p\, C_{Hr}\, U_r \left(\Theta_s - \Theta_r\right),\qquad (1b)$$

$$H_L = \rho\, L_v\, C_{Er}\, U_r \left(Q_s - Q_r\right).\qquad (1c)$$

Here, ρ is the air density; c_p, the specific heat of air at constant pressure; L_v, the latent heat of sublimation (if the surface is snow); U_r, Θ_r, and Q_r, respectively, the wind speed, potential temperature, and specific humidity at reference height r; Θ_s, the potential temperature at the surface; and Q_s, the specific humidity at the surface.

The crux of the bulk flux algorithm is evaluating the transfer coefficients for momentum, sensible heat, and latent heat appropriate at reference height r—respectively, C_{Dr}, C_{Hr}, and C_{Er} in (1). These generally derive from Monin-Obukhov similarity theory and formally are (e.g., Garratt 1992, p. 52ff.; Andreas 1998)

$$C_{Dr} = \frac{k^2}{\left[\ln\left(\dfrac{r}{z_0}\right) - \psi_m\left(\dfrac{r}{L}\right)\right]^2} ,\qquad (2a)$$

$$C_{Hr} = \frac{k^2}{\left[\ln\left(\dfrac{r}{z_0}\right) - \psi_m\left(\dfrac{r}{L}\right)\right]\left[\ln\left(\dfrac{r}{z_T}\right) - \psi_h\left(\dfrac{r}{L}\right)\right]} ,\qquad (2b)$$

$$C_{Er} = \frac{k^2}{\left[\ln\left(\dfrac{r}{z_0}\right) - \psi_m\left(\dfrac{r}{L}\right)\right]\left[\ln\left(\dfrac{r}{z_Q}\right) - \psi_h\left(\dfrac{r}{L}\right)\right]} .\qquad (2c)$$

Here, k (= 0.40) is the von Kármán constant, and ψ_m and ψ_h are empirical functions of the stability parameter r/L, where L is the Obukhov length. For ψ_m and ψ_h, we use Paulson's (1970) formulation for unstable stratification (i.e., $r/L < 0$) and Holtslag and De Bruin's (1988) for stable stratification (i.e., $r/L > 0$) (Jordan et al. 1999; Andreas 2002). Our measurements of and parameterizations for the roughness lengths for wind speed, temperature, and humidity over snow—z_0, z_T, and z_Q in (2)—are the subject of this paper.

Temperate snowpacks or continental surfaces sometimes do not satisfy the conditions of Monin-Obukhov similarity theory, however. Often the surface is not planar or horizontal. The diurnal cycle creates nonstationarity. The atmospheric flow may be disturbed by vegetation, topography, or structures and is, therefore, not horizontally homogeneous. Experimental evaluations of true z_0, z_T, and z_Q values in such conditions are consequently difficult.

Snow-covered sea ice, in contrast, provides a nearly ideal environment for measuring z_0, z_T, and

---

[*]*Corresponding author address:* Edgar L Andreas, U.S. Army Cold Regions Research and Engineering Laboratory, 72 Lyme Road, Hanover, NH 03755; e-mail: eandreas@crrel.usace.army.mil.

z_Q. The surface is planar, horizontal, and at sea level. The diurnal signal is often weak or nonexistent because of the low sun angle or the absence of the sun for long periods and because of the high reflectivity and high emissivity of the surface. Finally, sites in the central Arctic or Antarctic ice pack are uncomplicated by topography.

Values of z_0, z_T, and z_Q measured at such sea ice sites could be considered prototypical for all snow-covered surfaces and should yield parameterizations for the fundamental processes that control turbulent exchange over snow. At more complex sites, these fundamental processes should still operate. Although the local complexity of the site may require adjusting the roughness lengths, these canonical values of z_0, z_T, and z_Q should still be the right order of magnitude.

Here we use thousands of hours of eddy-correlation measurements made over snow-covered sea ice to evaluate such prototypical values of z_0, z_T, and z_Q. We then develop a new parameterization for z_0 as a function of the friction velocity u_* $[= (\tau/\rho)^{1/2}]$. Meanwhile, the z_T and z_Q values seem well represented by Andreas's (1987) theoretical model.

2. MEASUREMENTS

We use two large data sets for these analyses. One comes from Ice Station Weddell (ISW), which drifted through the western Weddell Sea from early February until early June 1992 (Gordon and Lukin 1992; ISW Group 1993; Andreas and Claffey 1995). The other comes from SHEBA (the experiment to study the Surface Heat Budget of the Arctic Ocean; Uttal et al. 2002), which was an ice camp deployed around the Canadian icebreaker *Des Groseilliers* that drifted in the Beaufort Gyre from early October 1997 until early October 1998.

On Ice Station Weddell, we used a three-axis ATI sonic anemometer/thermometer and an AIR Lyman-α hygrometer mounted on a tower at a height of 4.65 m to make eddy-correlation measurements of τ, H_s, and H_L in (1) (Andreas et al. 2004). We also had additional meteorological instruments for measuring the average quantities on the right sides of (1). These instruments ran almost continuously for over 2200 hours; we averaged their data into hourly values.

During SHEBA, our Atmospheric Surface Flux Group (ASFG) maintained five sites that measured τ and H_s by eddy correlation (Andreas et al. 1999, 2003; Persson et al. 2002). The main

site was our 20-m ASFG tower, which was instrumented at five heights between 2 and 18 m with ATI sonic anemometer/thermometers. Near the 9-m level on this tower, we also had an Ophir fast-responding hygrometer, which, when combined with the nearby sonic, yielded our sole SHEBA measurement of H_L.

At the other four SHEBA sites, we deployed portable automated mesonet (PAM) stations— these are the flux-PAM stations from NCAR's instrument pool (Militzer et al. 1995). These PAM stations featured either ATI or Gill sonic anemometer/thermometers mounted at heights between 2 and 4 m above the surface. We named our first four PAM sites Atlanta, Baltimore, Cleveland, and Florida after the teams playing in the Major League Baseball Championship Series in the fall of 1997 while we were building the SHEBA ice camp. The Atlanta, Baltimore, and Florida sites lasted for the entire experiment. A pressure ridge engulfed the Cleveland PAM station in late January 1998, and the station was offline for several months for refurbishing. We redeployed it at a site called Seattle in spring 1998 and, later in the summer, moved it to Maui.

Our main SHEBA tower and three of the PAM stations therefore ran almost continuously for about 8000 hours. The Cleveland/Seattle/Maui station had a shorter record. We again averaged the flux data and the associated mean meteorological quantities in (1) hourly. But here we focus on just the winter SHEBA period, when the sea ice was snow covered and the snow was dry enough to drift and blow (Andreas et al. 2003). We define "winter" at SHEBA as running from the start of the experiment in October 1997 through 14 May 1998. Winter resumed on 15 September 1998 and continued through the end of the deployment.

Since at ISW and SHEBA we directly measured all the terms in (1) except C_{Dr}, C_{Hr}, and C_{Er}, we can calculate these for each hour of good data. On rearranging (2), we can then use these measured coefficients to calculate z_0, z_T, and z_Q. That is,

$$z_0 = r \exp\left\{-\left[k C_{Dr}^{-1/2} + \psi_m\left(r/L\right)\right]\right\}, \quad (3a)$$

$$z_T = r \exp\left\{-\left[k C_{Dr}^{1/2} C_{Hr}^{-1} + \psi_h\left(r/L\right)\right]\right\}, \quad (3b)$$

$$z_Q = r \exp\left\{-\left[k C_{Dr}^{1/2} C_{Er}^{-1} + \psi_h\left(r/L\right)\right]\right\}. \quad (3c)$$

We, of course, screened the data we used in these calculations to ensure quality. For example, we excluded from the analysis small values of τ, H_s, and H_L, which do not have good signal-to-noise ratios when measured by eddy correlation. We generally measured Θ_s radiatively and evaluated Q_s as the saturation value at Θ_s. Because measuring these surface values over snow is difficult, we also excluded hours when $\left|\Theta_s - \Theta_r\right|$ or $\left|Q_s - Q_r\right|$ were small because of the large uncertainty in the resulting C_{Hr} and C_{Er} values. Finally, we excluded z_0, z_T, and z_Q values computed to be larger than 0.1 m and z_T and z_Q values computed to be smaller than 7×10^{-8} m, the nominal value for the mean free path of an air molecule. These constraints on z_0, z_T, and z_Q, however, did not eliminate many values.

3. THE ROUGHNESS LENGTH z_0

To provide you with an appreciation for the range of z_0 and u_* values in our data sets, Fig. 1 shows over 2500 measurements of z_0 from our main SHEBA tower. Although that tower had sonics at five levels, we averaged all good estimates of z_0 for any hour to obtain only one tower value per hour. (We do the same later with the z_T data.) The two features to notice in Fig. 1 are the wide scatter in z_0 values and their tendency to increase with u_*, the friction velocity.

For mobile surfaces such as sand and snow, an argument based on the conservation of mechanical energy suggests that z_0 should scale with u_*^2 / g, where g is the acceleration of gravity (Owen 1964; Chamberlain 1983; Pomeroy and Gray 1990). Presumably, this mechanism should operate only above the threshold at which saltation begins. From our observations of drifting snow on Ice Station Weddell (Fig. 2), we estimate this
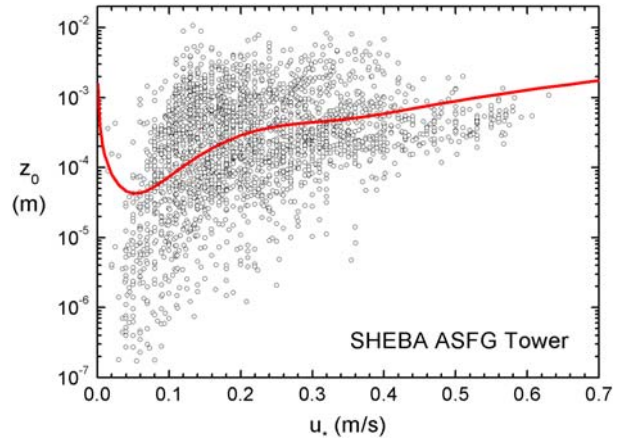

Figure 1. Hourly values of the roughness length for wind speed, z_0, as a function of the friction velocity, u_*, measured during winter at the SHEBA Atmospheric Surface Flux Group tower. The line is (4) with A = 1.
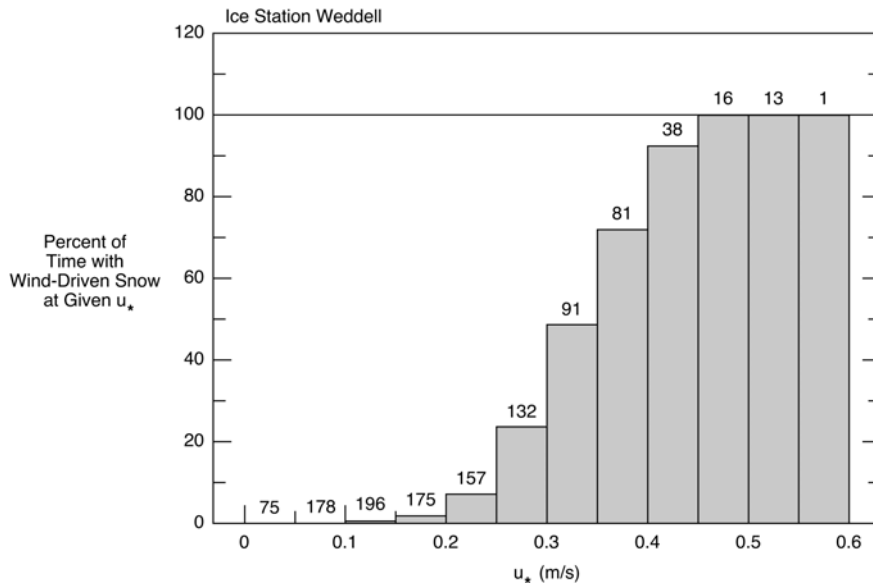

Figure 2. Observations of drifting and blowing snow on Ice Station Weddell for various u_* bins. The u_* values are hourly averages based on eddy-correlation measurements; the number above each histogram bar is the number of observations in that u_* bin.

3

threshold value of u_* to be about $0.3\,\mathrm{m\,s^{-1}}$. That is, this figure shows that the fraction of the time for which drifting and blowing snow was observed increases dramatically once u_* reaches $0.3\,\mathrm{m\,s^{-1}}$.

In light of this saltation mechanism, Jordan et al. (2001) and Andreas et al. (2003, 2004) proposed a formulation for z_0 in terms of u_* that includes a saltation regime and an aerodynamically smooth regime (Smith 1988), the latter like Fairall et al (1996, 2003) employed in the COARE air-sea bulk flux algorithm. Our current algorithm is

$$z_0 = \frac{0.135\,\nu}{u_*} + \frac{0.035\,u_*^2}{g}\left\{1 + A\exp\left[-\left(\frac{u_* - 0.18}{0.10}\right)^2\right]\right\}, \quad (4)$$

where ν is the kinematic viscosity of air, and z_0 is in meters when u_* is in $\mathrm{m\,s^{-1}}$. The left-most term on the right side of (4) models the aerodynamically smooth regime. The 1 in curly brackets, when multiplied by $0.035\,u_*^2/g$, models the saltation regime for u_* values above about $0.3\,\mathrm{m\,s^{-1}}$. The exponential term in (4), we believe, reflects the "fundamental" roughness of the surface because A is a dimensionless coefficient that varies among sites.

Figure 3 shows all of our SHEBA z_0 values averaged in u_* bins that are typically $2\,\mathrm{cm\,s^{-1}}$ wide. The points in this plot represent over 9400 hours of data. Except for Cleveland and Maui, which had shorter lifetimes, each point in Fig. 3 typically represents about 100 hours of data for the given u_* bin.
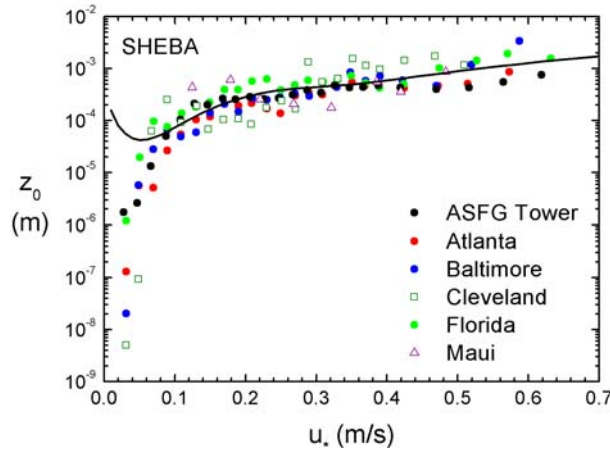
The line in Fig. 3 is (4) with $A = 1$. For u_* values above $0.08\,\mathrm{m\,s^{-1}}$, this line is roughly within half an order of magnitude of all of our bin-averaged SHEBA z_0 values. The SHEBA data, however, fall far below (4) at small u_*. We frankly have no good explanation for this behavior. Laboratory data repeatedly confirm that z_0 scales with ν/u_* when u_* is small, and the data that Fairall et al. (2003) reported for the open ocean likewise suggest that z_0 increases at small u_*, as (4) predicts. Further, we can think of no physical reason for z_0 to be as small as 10^{-6}–10^{-7} over snow-covered sea ice. Our best explanation is that our measurements or analysis are not correct when u_* is small. For instance, the stability corrections—represented by ψ_m and ψ_h in (3a)—may not be accurate in the very stable stratification usually associated with small u_* values over polar sea ice. Or perhaps in this very stable stratification, the boundary layer is so shallow that an eddy-correlation measurement of τ several meters above the surface is much smaller than the true surface flux.

Figure 4 shows comparable bin-averaged z_0 values from Ice Station Weddell. Besides the eddy-correlation measurements on ISW that we already described, the figure also includes z_0 values that Andreas and Claffey (1995) obtained from wind speed profiles measured on ISW. The z_0 values in Fig. 4 represent 197 hours of profile measurements and over 700 hours of eddy-correlation measurements.
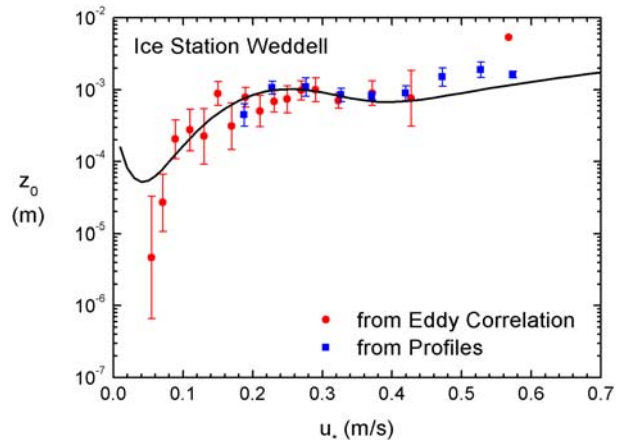

Figure 3. Bin-averaged values of z_0 from our main SHEBA tower and from five SHEBA flux-PAM sites. The line is (4) with $A = 1$.

Figure 4. Bin-averaged values of z_0 from both eddy-correlation and wind speed profile measurements on Ice Station Weddell. The error bars are ± 2 standard deviations of the mean z_0 values. The line is (4) with $A = 5$.

4

The line in Fig. 4 is again (4) but with A = 5. That is, the "fundamental" roughness of the surface at Ice Station Weddell seems to have been larger than at SHEBA. In fact, Fig. 4 suggests a local maximum in roughness in the vicinity of $u_* = 0.25 \, \mathrm{m \, s^{-1}}$. Andreas and Claffey (1995) and Andreas (1995) attribute this local maximum to sastrugi that build during storm winds, when u_* is above the threshold for drifting and blowing snow. When the storm passes and the winds decline, they usually turn and thereby see a corrugated surface that is aerodynamically rougher than if the wind were blowing parallel to the sastrugi. In contrast, we never observed much sastrugi building during SHEBA.

4. THE SCALAR ROUGHNESS LENGTHS

4.1 Background

Andreas (1987) developed a theoretical model for z_T/z_0 and z_Q/z_0 that is still the only prediction for how z_T and z_Q behave over snow-covered surfaces. The main result from that model is

$$z_s / z_0 = \exp\left[b_0 + b_1 \left(\ln R_* \right) + b_2 \left(\ln R_* \right)^2 \right], \quad (5)$$

where z_s is the scalar roughness—either z_T or z_Q—and $R_* = u_* z_0 / \nu$ is the roughness Reynolds number. Table 1 gives the coefficients b_0, b_1, and b_2 in the model.

In his review of scalar transfer over snow and ice surfaces, Andreas (2002) compared z_T values from several modestly sized data sets against the predictions from (5) and found they generally agreed. Andreas, however, found only one small data set for likewise testing how (5) does at predicting z_Q. This comparison showed large differences between the z_Q measurements and the prediction, presumably because the z_Q data were not very good. Meanwhile, based on profile measurements in Queen Maud Land, Antarctica, Bintanja and Reijmer (2001) reported z_T and z_Q values over show that showed a very strong dependence on u_*—a dependence incompatible with Andreas's (1987) model, (5). We here bring to bear on this discussion many new measurements of z_T and z_Q from SHEBA and from Ice Station Weddell.

4.2 The Roughness Length z_T

Common practice is to scale z_T with z_0 (e.g., Garratt and Hicks 1973). In fact, Andreas's (1987) theory predicts z_T/z_0 and z_Q/z_0 rather than z_T and z_Q individually. Figure 5 shows how individual estimates of z_T/z_0 from (3a) and (3b) can vary. The data in the figure do, nevertheless, tend to corroborate (5).

As with Figs. 3 and 4, because of the scatter in individual measurements of the roughness length, we like to bin average. Figure 6 therefore shows z_T/z_0 values averaged in R_* bins for five SHEBA sites and for Ice Station Weddell. The

Table 1. Values of the coefficients to use in (5) for estimating z_T/z_0 and z_Q/z_0 in three aerodynamic regions.

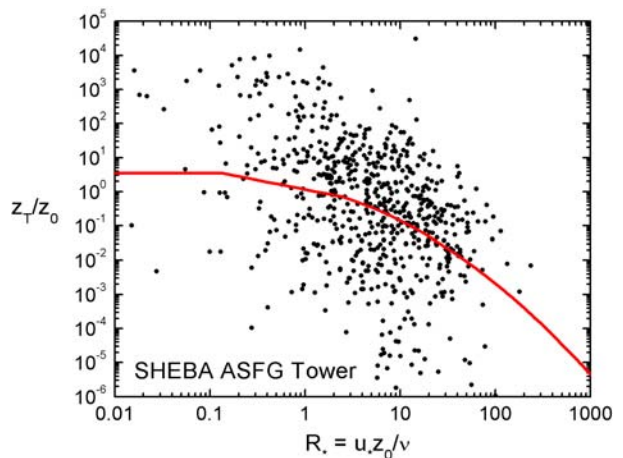|	$R_* \leq 0.135$ Smooth	$0.135 < R_* < 2.5$ Transition	$2.5 \leq R_* \leq 1000$ Rough
Temperature (z_T/z_0)			
b_0	1.250	0.149	0.317
b_1	0	−0.550	−0.565
b_2	0	0	−0.183
Humidity (z_Q/z_0)			
b_0	1.610	0.351	0.396
b_1	0	−0.628	−0.512
b_2	0	0	−0.180

Figure 5. Hourly values of z_T/z_0 measured on the Atmospheric Surface Flux Group's tower at SHEBA and parameterized with the roughness Reynolds number. The line is (5).
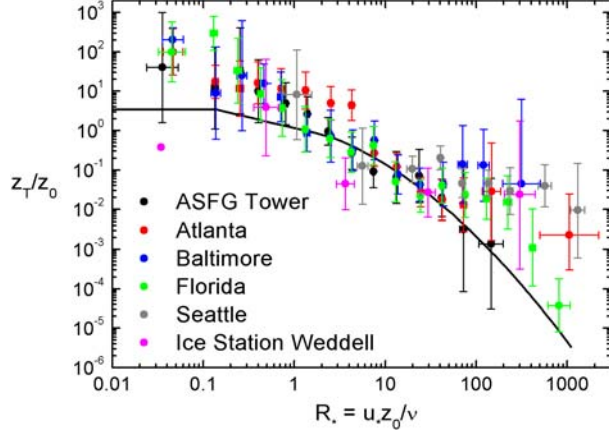
Figure 6. Hourly values of z_T/z_0 from our main SHEBA tower, from the SHEBA flux-PAMs at Atlanta, Baltimore, Florida, and Seattle, and from Ice Station Weddell are averaged in R_* bins. The error bars are ±2 standard deviations of the means of z_T/z_0 and R_*. The points without error bars are individual values. The line is (5).

Figure 7. The same z_T data from Fig. 6 are here averaged in u_* bins. The error bars are ±2 standard deviations of the means of z_T and u_*. The line results from combining (5) with (4) and using A = 1 in (4).

points in this plot represent over 2200 hourly z_T measurements.

One essential conclusion from this plot is that, in general, $z_T \neq z_0$, while $z_T = z_Q = z_0$ is a common assumption in snow models (e.g., Bryan et al. 1996; Martin and Lejeune 1998). Another conclusion from Fig. 6 is that Andreas's (1987) model, (5), does pretty well in representing the z_T/z_0 values, especially in the transition region, $0.135 < R_* < 2.5$, and in the aerodynamically rough region, $R_* \geq 2.5$. The figure does, however, suggest that the predictions from (5) may be low in aerodynamically smooth flow, $R_* \leq 0.135$, and in very rough flow, $R_* > 200$. The behavior of the data for small R_* may, however, again be a consequence of measurement or analysis biases in very stable stratification. We have not decided yet whether the relatively large z_T/z_0 values for large R_* are real or are a measurement artifact.

Andreas (2002) and Andreas et al. (2004) raised the issue that plots of z_T/z_0 and z_Q/z_0 versus $R_* = u_* z_0 / \nu$ may suffer from fictitious correlation because of the shared z_0. Andreas (2002), in fact, showed with one example that this built-in correlation tends to make z_T/z_0 decrease with increasing R_*, as both the model and the data suggest in Fig. 6. To remove this fictitious correlation, we therefore plot in Fig. 7 values of z_T alone averaged in u_* bins.

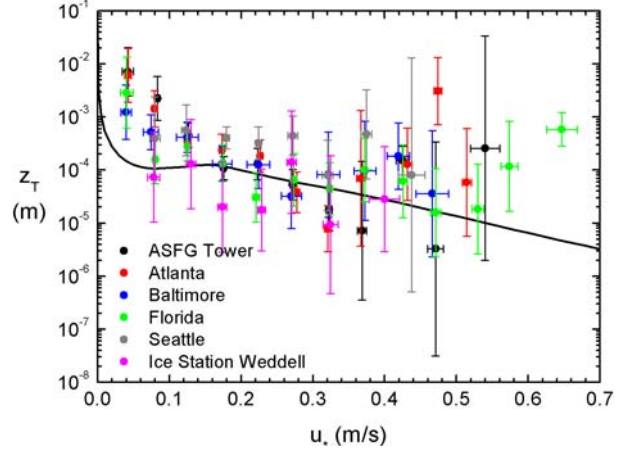The line in Fig. 7 results from combining (4) and (5), with A = 1 in (4). This line does pretty well

in representing the z_T values, except again for very small u_*, where we may have measurement or analysis problems. The results in Fig. 7 are also compatible with a constant z_T value of about 1×10^{-4} m. Figure 7, however, does not corroborate the finding by Bintanja and Reijmer (2001) that z_T increases as a high power of u_* for u_* above a saltation threshold of about $0.3 \, \mathrm{m\,s^{-1}}$.

4.3 The Roughness Length z_Q

Figure 8 shows about 160 bin-averaged z_Q/z_0 values measured on our SHEBA ASFG tower and on Ice Station Weddell. The values agree quite well with Andreas's (1987) model, (5), and provide the first meaningful test of his theory for humidity roughness. Once again, the disagreement between measurements and the prediction for small R_* may result from either a measurement or analysis problem. But this disagreement could also point to a shortcoming in Andreas's model.

As with z_T/z_0, plots of z_Q/z_0 versus R_* can suffer from fictitious correlation because of the shared z_0. Therefore, Fig. 9 shows averaged values of z_Q alone in u_* bins. The line in this figure again derives from (4) and (5), with A = 5 in (4), and splits the plotted averages. Nevertheless, the data in Fig. 9 are not precise enough for us to reject the hypothesis that z_Q over snow in the u_* range depicted is constant with a value that is, nominally, 1×10^{-4} m.
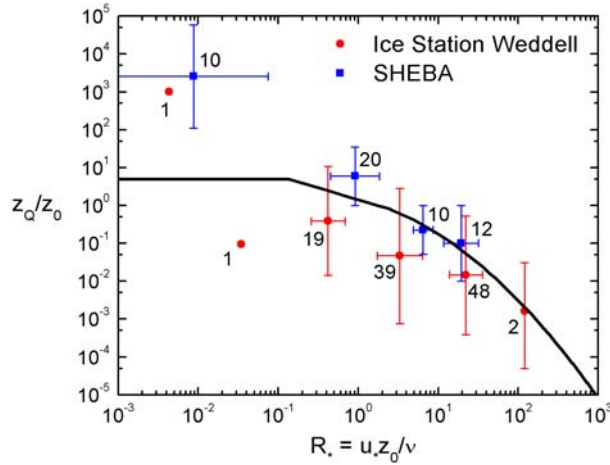
Figure 8. Hourly values of z_Q/z_0 from the SHEBA ASFG tower and from Ice Station Weddell are averaged in R_* bins. The error bars are ± 2 standard deviations of the means of the z_T/z_0 and R_* values in the bin; the numbers beside the markers tell the number of values in each bin. The line is (5).
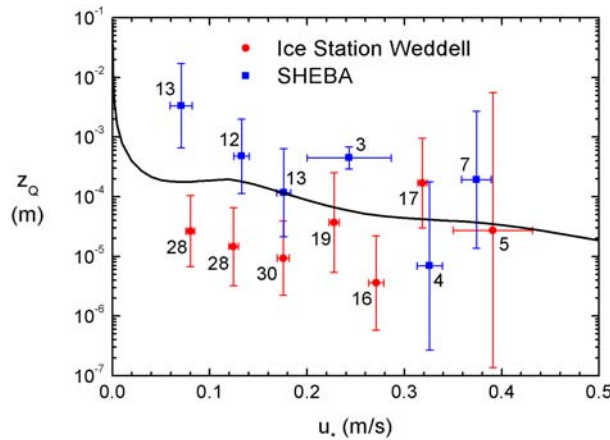

Figure 9. The same z_Q data in Fig. 8 are here averaged in u_* bins. The error bars are ± 2 standard deviations of the means of the z_Q and u_* values for the bin; the numbers beside the markers tell the number of values in each bin. The line results from combining (4) and (5), with A = 5 in (4).

5. CONCLUSIONS

Our turbulent flux and associated meteorological measurements during SHEBA and on Ice Station Weddell provided thousands of new measurements of the roughness lengths z_0, z_T, and z_Q for snow-covered surfaces. On the basis of these data, we developed a new parameterization

for z_0, equation (4), that acknowledges three regimes: an aerodynamically smooth regime for small u_*, where z_0 scales with ν/u_*; a drifting and blowing snow regime for large u_*, where z_0 scales with u_*^2/g; and an intermediate regime between these two extremes, where the "fundamental" roughness of the surface dictates z_0. By adjusting only one coefficient in this parameterization, we were able to fit both the SHEBA and Ice Station Weddell data for u_* up to $0.7\,\mathrm{m\,s^{-1}}$.

Both the SHEBA and Ice Station Weddell z_T and z_Q values tend to corroborate Andreas's (1987) theoretical model for z_T/z_0 and z_Q/z_0. But we see that most of the variations in z_T/z_0 and z_Q/z_0 result from variations in z_0. The z_T and z_Q values alone, in contrast, seem to be fairly constant, with a common value of about $1\times10^{-4}\,\mathrm{m}$.

Because snow-covered sea ice is such a prototypical site for investigating the fundamental behavior of turbulent exchange over snow, the z_0, z_T, and z_Q values that we have reported should constrain measurements and parameterizations for these roughness lengths over snow at more complex sites.

6. ACKNOWLEDGMENTS

7. REFERENCES

Andreas, E. L, 1987: A theory for the scalar roughness and the scalar transfer coefficients over snow and sea ice. *Bound.-Layer Meteor.*, **38**, 159–184.

_____, 1995: Air-ice drag coefficients in the western Weddell Sea: 2. A model based on form drag and drifting snow. *J. Geophys. Res.*, **100**, 4833–4843.

_____, 1998: The atmospheric boundary layer over polar marine surfaces. *Physics of Ice-Covered Seas, Vol. 2*, M. Leppäranta, Ed., Helsinki University Press, 715–773.

_____, 2002: Parameterizing scalar transfer over snow and ice: A review. *J. Hydrometeor.*, **3**, 417–432.

——, and K. J. Claffey, 1995: Air-ice drag coefficients in the western Weddell Sea: 1. Values deduced from profile measurements. *J. Geophys. Res.*, **100**, 4821–4831.

——, C. W. Fairall, P. S. Guest, and P. O. G. Persson, 1999: An overview of the SHEBA atmospheric surface flux program. Preprints, *Fifth Conf. on Polar Meteorology and Oceanography*, Dallas, TX, Amer. Meteor. Soc., 411–416.

——, ——, A. A. Grachev, P. S. Guest, T. W. Horst, R. E. Jordan, and P. O. G. Persson, 2003: Turbulent transfer coefficients and roughness lengths over sea ice: The SHEBA results. CD-ROM of preprints, *7th Conf. on Polar Meteorology and Oceanography*, Hyannis, MA, Amer. Meteor. Soc., 9 pp.

——, R. E. Jordan, and A. P. Makshtas, 2004: Parameterizing turbulent exchange over sea ice: The Ice Station Weddell results. *Bound.-Layer Meteor.*, submitted.

Bintanja, R., 2000: Surface heat budget of Antarctic snow and blue ice: Interpretation of spatial and temporal variability. *J. Geophys. Res.*, **105**, 24,387–24,407.

Bintanja, R., and C. H. Reijmer, 2001: A simple parameterization for snowdrift sublimation over Antarctic snow surfaces. *J. Geophys. Res.*, **106**, 31,739–31,748.

Brun, E., E. Martin, V. Simon, C. Gendre, and C. Coleou, 1989: An energy and mass model of snow cover suitable for operational avalanche forecasting. *J. Glaciol.*, **35**, 333–342.

Bryan, F. O., B. G. Kauffman, W. G. Large, and P. R. Gent, 1996: The NCAR CSM flux coupler. NCAR Tech. Note NCAR/TN-424+STR, 48 pp.

Chamberlain, A. C., 1983: Roughness length of sea, sand, and snow. *Bound.-Layer Meteor.*, **25**, 405–409.

Fairall, C. W., E. F. Bradley, D. P. Rogers, J. B. Edson, and G. S. Young, 1996: Bulk parameterization of air-sea fluxes for Tropical Ocean-Global Atmosphere Coupled-Ocean Atmosphere Response Experiment. *J. Geophys. Res.*, **101**, 3747–3764.

——, ——, J. E. Hare, A. A. Grachev, and J. B. Edson, 2003: Bulk parameterization of air-sea fluxes: Updates and verification for the COARE algorithm. *J. Climate*, **16**, 571–591.

Garratt, J. R., 1992: *The Atmospheric Boundary Layer*. Cambridge University Press, 316 pp.

Garratt, J. R., and B. B. Hicks, 1973: Momentum, heat and water vapour transfer to and from natural and artificial surfaces. *Quart. J. Roy. Meteor. Soc.*, **99**, 680–687.

Gordon, A. L., and V. V. Lukin, 1992: Ice Station Weddell #1. *Antarct. J. U. S.*, **27** (5), 97–99.

Holtslag, A. A. M., and H. A. R. De Bruin, 1988: Applied modeling of the nighttime surface energy balance over land. *J. Appl. Meteor.*, **27**, 689–704.

ISW Group, 1993: Weddell Sea exploration from ice station. *Eos, Trans. Amer. Geophys. Union*, **74**, 121–126.

Jordan, R. E., E. L Andreas, and A. P. Makshtas, 1999: Heat budget of snow-covered sea ice at North Pole 4. *J. Geophys. Res.*, **104**, 7785–7806.

——, ——, and ——, 2001: Modeling the surface energy budget and the temperature structure of snow and brine-snow at Ice Station Weddell. Preprints, *Sixth Conf. on Polar Meteorology and Oceanography*, San Diego, CA, Amer. Meteor. Soc., 129–132.

Martin, E., and Y. Lejeune, 1998: Turbulent fluxes above the snow surface. *Ann. Glaciol.*, **26**, 179–183.

Militzer, J. M., M. C. Michaelis, S. R. Semmer, K. S. Norris, T. W. Horst, S. P. Oncley, A. C. Delany, and F. V. Brock, 1995: Development of the prototype PAM III/Flux-PAM surface meteorological station. Preprints, *9th Symp. on Meteorological Observations and Instrumentation*, Charlotte, NC, Amer. Meteor. Soc., 490–494.

Owen, P. R., 1964: Saltation of uniform grains in air. *J. Fluid Mech.*, **20**, 225–242.

Paulson, C. A., 1970: The mathematical representation of wind speed and temperature profiles in the unstable atmospheric surface layer. *J. Appl. Meteor.*, **9**, 857–861.

Persson, P. O. G., C. W. Fairall, E. L Andreas, P. S. Guest, and D. K. Perovich, 2002: Measurements near the Atmospheric Surface Flux Group tower at SHEBA: Near-surface conditions and surface energy budget. *J. Geophys. Res.*, **107** (C10), DOI: 10.1029/2000JC000705.

Pomeroy, J. W., and D. M. Gray, 1990: Saltation of snow. *Water. Resour. Res.*, **26**, 1583–1594.

Smith, S. D., 1988: Coefficients for sea surface wind stress, heat flux, and wind profiles as a function of wind speed and temperature. *J. Geophys. Res.*, **93**, 15,467–15,472.

Uttal, T., and 27 others, 2002: Surface Heat Budget of the Arctic Ocean. *Bull. Amer. Meteor. Soc.*, **83**, 255–275.